ELSEVIER

Electrochemistry Communications 4 (2002) 727–731

electrochemistry communications

www.elsevier.com/locate/elecom

Synthesis of nano-crystalline $LiFeO_2$ material with advanced battery performance

Yun Sung Lee [a], Chong Seung Yoon [b], Yang Kook Sun [c], Koichi Kobayakawa [d], Yuichi Sato [d,*]

[a] *High-Tech Research Center, Kanagawa University, 3-27-1 Rokkakubashi, Yokohama 221-8686, Japan*
[b] *Division of Material Science and Engineering, Hanyang University, 17 Haengdang-dong, Seoul 133-791, Republic of Korea*
[c] *Department of Chemical Engineering, Hanyang University, 17 Haengdang-dong, Seoul 133-791, Republic of Korea*
[d] *Department of Applied Chemistry, Kanagawa University, 3-27-1 Rokkakubashi, Yokohama 221-8686, Japan*

Received 15 July 2002; received in revised form 23 July 2002; accepted 31 July 2002

Abstract

$LiFeO_2$ has been synthesized at low temperature (150 °C) using the solid-state method. It was composed of orthorhombic $LiFeO_2$ and small amount of spinel $LiFe_5O_8$ phases. A $Li/LiFeO_2$ cell showed not only a fairly high initial discharge capacity of over 150 mAh/g, but also a good cycle retention rate at room temperature. During the cycling test, the $Li/LiFeO_2$ cell exhibited a unique abrupt capacity drop near the 13th cycle and continuously showed an excellent cycling performance of over 99% for 25 cycles. We found that the orthorhombic $LiFeO_2$ underwent a structural change to the spinel phase during the charge/discharge process which resulted in the capacity decline during the long-term cycling. © 2002 Elsevier Science B.V. All rights reserved.

Keywords: Orthorhombic; $LiFeO_2$; Nano-crystalline; Abrupt capacity drop; Lithium secondary batteries

1. Introduction

The commercial lithium battery with high energy density and good cycle life has been studied as a power source for portable electronics. Many research groups have investigated various cathode materials for the lithium secondary batteries such as a layered oxide; $LiMO_2$ (M = Co, Ni, Mn, Fe), which consists of alternating layers of trigonally distorted MO_6 and LiO_6 octahedral sharing edges [1–6].

$LiCoO_2$ has many problems such as high cost, environmental concerns and low practical capacity (about 130 mAh/g) [1,2]. Although $LiNiO_2$ has a higher practical capacity than $LiCoO_2$, it is highly possible that exothermic decomposition of the oxide will occur by releasing oxygen at high temperature [3,4]. $LiMnO_2$ still shows a small discharge capacity in the 4 V region which is a problem for commercialization it, especially the orthorhombic type, because of the increasing initial discharge capacity in the early stage [5,6].

$LiFeO_2$ has many advantages over these layered cathode materials because it is nontoxic and contains the most abundant metal in the world. It is well known that $LiFeO_2$ has different forms, i.e, the α-, β-, and γ-forms, due to the synthetic conditions and synthetic method. The α-$LiFeO_2$ is a cubic unit cell of space group Fm3m, β-$LiFeO_2$ (monoclinic, C2/c) is formed by an intermediate phase during the ordering process. The γ-$LiFeO_2$ (tetragonal, $I4_1/amd$) is obtained by reducing the symmetry from cubic to tetragonal by ordering the Li^+ and Fe^{3+} ions at octahedral sites [7–15].

Kanno et al. [7,8] found that the corrugated layered structure $LiFeO_2$ compound was electrochemically active during the lithium insertion/extraction reaction. They noticed one interesting point that orthorhombic $LiMnO_2$ using LiOH and γ-MnOOH, which has a structure similar to the conjugated $LiFeO_2$, was successfully synthesized by an ion exchange method at low temperature [16,17]. They succeeded in synthesizing $LiFeO_2$ using the H^+/Li^+ ion exchange reaction from

* Corresponding author. Fax: +81-45-508-7480.
E-mail address: satouy01@kanagawa-u.ac.jp (Y. Sato).

1388-2481/02/$ - see front matter
PII: S1388-2481(02)00436-8

γ-FeOOH at a reaction temperature of 100–500 °C. Although this $Li/LiFeO_2$ cell exhibited a fairly high initial discharge capacity of about 100 mAh/g and lithium reversibly inserts/extracts in the FeO_2 layers, it shows a large capacity decline due to the cationic disorder in the voltage region of 4.2 and 1.5 V.

Tabuchi et al. [9–13] reported many interesting results for all types of $LiFeO_2$ compounds. They successfully adopted a new synthetic process, the hydrothermal method, for the $LiFeO_2$ system. Many kinds of starting materials (α-FeOOH, $FeCl_3$, $Fe(NO_3)_3$, LiOH, NaOH, and KOH) at various Li/Fe (1–50) ratios were distilled in a Teflon beaker and hydrothermally treated at 230 °C in an autoclave. Although the α-$LiFeO_2$ derivatives were successfully obtained from α-FeOOH (Fe^{3+} source) and LiOH by a one-step method, the cycling performance of the α-$LiFeO_2$ compound was very poor (5–10 mAh/g) in the range 4.5–1.5 V.

However, Sakurai et al. [14] recently reported a new result that the corrugated $LiFeO_2$ material, which in synthesized by a H^+/Li^+ ion exchange method, could be easily obtained at low temperature when alcohol used as the reaction medium in the synthetic process. Furthermore, they succeeded in synthesizing another electrically active form of α-$LiFeO_2$ material, which is known to be very difficult to insert/extract lithium into and out of the structure, by reacting LiOH and α-FeOOH in 2-phenoxyethanol. Although this $Li/$α-$LiFeO_2$ cell delivered a small discharge capacity of 50 mAh/g after 50 cycles, it is a fairly good cycling result if we consider the electrochemical characteristics of the α-$LiFeO_2$ compound [15].

From a review of previous studies, we found that almost all $LiFeO_2$ materials were obtained using a complex reaction mechanism (e.g., ion exchange reaction, hydrothermal method). It needed a long reaction time or other reaction steps against the conventional solid-state method. Moreover, almost all the $LiFeO_2$ materials using these methods were unsatisfactory as a practical cathode material, from the viewpoint of a reversible discharge capacity and cycling performance, in lithium secondary batteries.

Therefore, we report here a new and easy synthetic method of orthorhombic $LiFeO_2$ with good battery performances using a conventional solid-state reaction at low temperature and present the unique cycling behavior of the orthorhombic $LiFeO_2$ material.

2. Experimental

$LiFeO_2$ was synthesized using $LiOH \cdot H_2O$ (Kishida Chemical, Japan), γ-FeOOH (High Purity Chemicals, Japan) by conventional solid-state method. The stoichiometric amount of each material was grounded and calcined at 150 °C for 15 h in argon atmosphere in the box furnace. The contents of Li and Fe in the resulting material were analyzed with atomic absorption spectroscopy (AAS, AA-6200, Shimadzu, Japan) by dissolving the powder in the dilute nitric acid.

The powder X-ray diffraction (XRD, Rint 1000, Rigaku, Japan) using CuKα radiation was employed to identify the crystalline phase of the synthesized material. To investigate the structural difference of the positive electrode before and after capacity drop, each tested cell was left in a glove box for 2 days to reach equilibrium after the cycling. The electrodes after cycling were washed with DMC solution to remove $LiPF_6$ salt. The particle morphology of $LiFeO_2$ material was observed using a scanning electron microscope (SEM, S-4000, Hitachi, Japan). Transmission electron microscope (TEM, JEM 2010, JEOL, Japan) equipped with energy-dispersive X-ray spectrometer (EDS) was employed to characterize the microstructure of powder.

The electrochemical characterizations were performed using CR2032 coin-type cell. The cathode was fabricated with 20 mg of accurately weighed active material and 12 mg of conductive binder (8 mg of Teflonized acetylene black (TAB) and 4 mg of graphite). It was pressed on 200 mm^2 stainless steel mesh used as the current collector under a pressure of 300 kg/cm^2 and dried at 130 °C for 5 h in an oven. The test cell was made of a cathode and a lithium metal anode (Cyprus Foote Mineral) separated by a porous polypropylene film (Celgard 3401). The electrolyte used was a mixture of 1 M $LiPF_6$–ethylene carbonate (EC)/dimethyl carbonate (DMC) (1:2 by vol., Ube Chemicals, Japan). The charge and discharge current density was 0.4 mA/cm^2 (or 0.1 mA/cm^2) with a cut-off voltage of 1.5–4.5 V at room temperature.

3. Results and discussion

To synthesize orthorhombic $LiFeO_2$ (herein referred to as *o*-$LiFeO_2$) by a conventional solid-state reaction, two mixtures of the LiOH and γ-FeOOH starting materials were thoroughly ground for 20 min in a mortar. One was calcined in a ceramic boat without pressing; the other was pressed at a 300 kg/cm^2 pressure into a 20 mm diameter pellet to improve the reactivity between the particles of the precursor.

Fig. 1 shows X-ray diffraction patterns (XRD) of the raw γ-FeOOH and the two $LiFeO_2$ materials which were calcined at 150 °C for 15 h in an Ar atmosphere. The $LiFeO_2$ mixture without pressing (Fig. 1(b)) shows a very similar XRD pattern when compared to the γ-FeOOH. It seems to have failed to form an orthorhombic structure, although there are some differences versus that of the original γ-FeOOH, which resulted from the reaction with lithium hydroxide at 80 °C. On the other hand, Fig. 1(c) displays a well-defined orthorhombic pattern in the XRD diagram. The characteristic

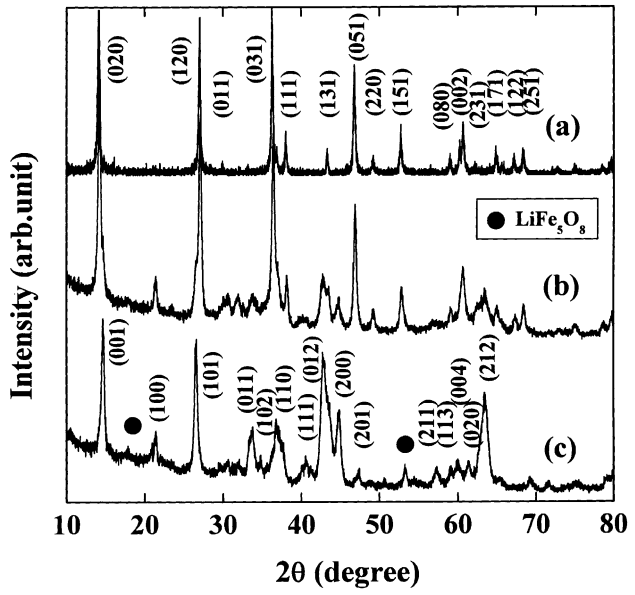

Fig. 1. X-ray diffraction patterns of (a) γ-FeOOH, (b) $LiFeO_2$ without pressing, and (c) $LiFeO_2$ with pressing.

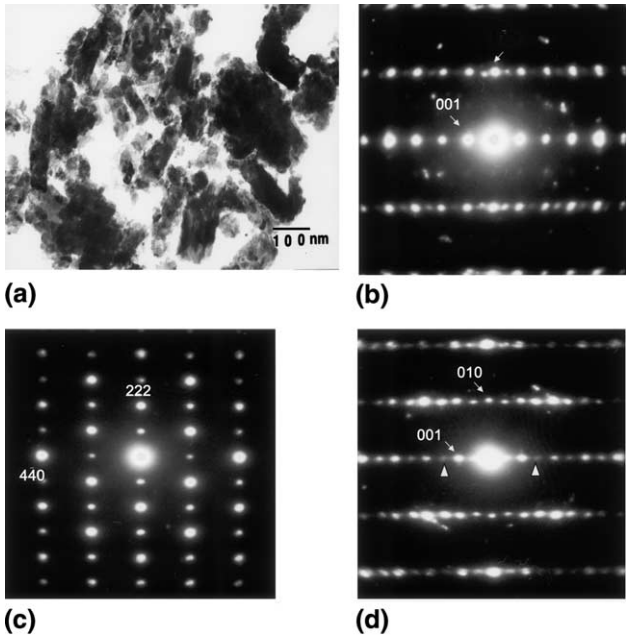

Fig. 2. TEM image and SAD patterns of resulting powder: (a) bright field image of orthorhombic $LiFeO_2$, (b) orthorhombic $LiFeO_2$ in [1 1 0] direction, (c) spinel β-$LiFe_5O_8$ in [1 1 2] direction, and (d) defective $LiFeO_2$ in [1 0 0] direction.

indications of the *o*-$LiFeO_2$ material are the well-defined split between the (0 1 1) and (1 1 0) peaks and between the (0 1 2) and (2 0 0) peaks, although there is a small amount of β-$LiFe_5O_8$ impurities. We found that the pelletizing in this study played an important role in accelerating the slow reaction of lithium and γ-FeOOH particles because the rate of the surface reaction of two starting materials slowly occurred at a low synthesis temperature.

Kanno et al. already reported that $LiFeO_2$ made from LiOH and γ-FeOOH (1:1) calcined for 1 h at the reaction temperature of 150 °C was composed of three kinds of phases, i.e., α-$LiFeO_2$, an unknown phase, and β-$LiFe_5O_8$. Even though they controlled the synthesis conditions (low vapor pressure) to obtain pure orthorhombic $LiFeO_2$ without α-$LiFeO_2$, the best sample still contained about 23% of the α-$LiFeO_2$ impurity in the $LiFeO_2$ powder. Fig. 2 shows the transmission electron microscope (TEM) bright field image and selected area electron diffraction (SAD) patterns of the *o*-$LiFeO_2$ material. All the electron diffraction patterns were obtained from the *o*-$LiFeO_2$ particle in this study. It shows that the $LiFeO_2$ sample consisted of 100–200 nm sized needle-type particles. It is composed of an orthorhombic phase ($a = 4.0$ Å, $b = 3.0$ Å, and $c = 6.1$ Å) with a small amount of β-$LiFe_5O_8$ ($a = 8.3$ Å) phase (Fig. 1(c)). Additionally, some of the orthorhombic phases (Fig. 2(d)) had different stacking sequencing in the *c*-direction, giving rise to the superlattice peak. The white arrows indicate the spots arising from the superlattice generated by the altered stacking sequence in the c-direction as shown above. We assume that the altered stacking sequence and higher spinel phase amount have combined to decrease the discharge capacity of the $LiFeO_2$ material. From the TEM analysis, it was found that the $LiFeO_2$ powder in this study was mixed with well-crystallized orthorhombic $LiFeO_2$, β-$LiFe_5O_8$, and defective $LiFeO_2$ phases.

Fig. 3 shows the charge/discharge curves for Li/1 M $LiPF_6$–EC/DMC/$LiFeO_2$ calcined at 150 °C for 15 h in

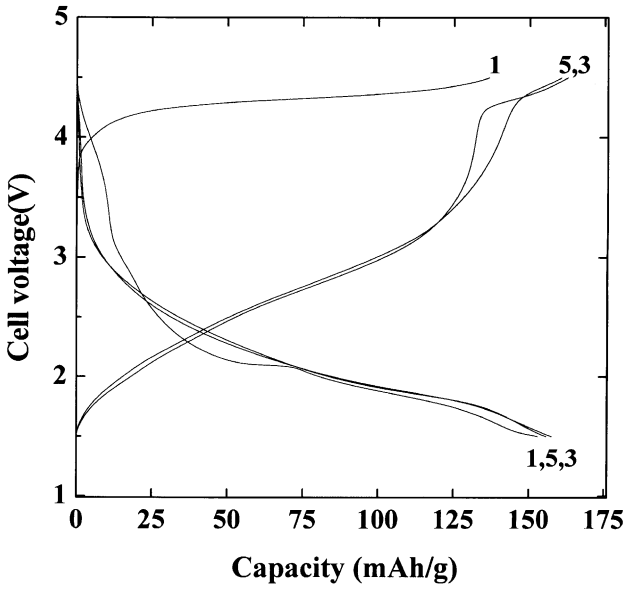

Fig. 3. The charge/discharge curves for the Li/1 M $LiPF_6$–EC/DMC/$LiFeO_2$ calcined at 150 °C for 15 h in argon. The test condition was a current density of 0.1 mA/cm^2 between 4.5 and 1.5 V at room temperature.

an argon atmosphere. The test condition was a current density of 0.1 mA/cm^2 between 4.5 and 1.5 V. The first charge of the Li/$LiFeO_2$ cell rapidly increased to 4.0 V and showed a plateau region between 4.2 and 4.3 V. While the first discharge curve abruptly decreased below 3.0 V and displayed a voltage plateau in the 2.0–2.1 V region followed by two more small voltage steps. From the second cycle, the plateau region in the 2.0 V region was not detected and it exhibited a slightly different cycle behavior. The initial discharge capacity of the Li/$LiFeO_2$ cell was 150 mAh/g, which was one of the previously reported largest values. Actually, the Li/$LiFeO_2$ cell in this study could insert lithium into the Li_xFeO_2 structure up to 259 mAh/g ($x = 1.92$) at the very low current density of 0.01 mA/cm^2. We assume that the large discharge capacity of Li/$LiFeO_2$ cell in this study might result from the absence (or scarcity) of the inactive α-$LiFeO_2$ impurity in the $LiFeO_2$ structure and its small nano-sized particles improved the structural stability of $LiFeO_2$ powders during cycling process.

Fig. 4 shows the variation in the specific discharge capacity with the number of cycles for the $LiFeO_2$ material. The current density was 0.4 mA/cm^2 between 4.5 and 1.5 V. The Li/$LiFeO_2$ cell exhibited a very excellent cycle performance until the 13th cycle; however, the discharge capacity abruptly decreased about 8.2% of the capacity at the 14th cycle and it again showed very stable cycling to 25 cycles. The cycle retention rate was 97% from the 1st to 13th cycles and 99.4% from the 13th to 25th cycles. This indication was perfectly reproduced in other test cells. We suggest that it can be one characteristic of the $LiFeO_2$ material obtained by the solid-state synthesis method at low temperature.

In order to investigate the unique cycling behavior observed with the Li/$LiFeO_2$ cell before and after the 13th cycle, ex situ XRD measurements were taken of four $LiFeO_2$ electrodes in the discharged state after various cycles as shown in Fig. 5. Each cell was left in a glove box for 2 days to reach equilibrium after being tested from 1.5 to 4.5 V. Unfortunately, it was impossible to detect a significant difference in the XRD in two electrodes between the 10th cycle and 15th cycle because of the very low crystallinity after cycling. However, it has been found that there are two main differences. First was the change in the (0 0 1) peak about $2\theta = 14.6°$, which is a characteristic peak of the orthorhombic structure in the XRD diagram. As the cycling proceeded, the intensity of the (0 0 1) peak gradually decreased. Second, the Li/$LiFeO_2$ cell showed a gradual capacity loss after 25 cycles and the cycle retention rates after 50 cycles were 73.4% (82% from capacity drop on 13th cycle). Moreover, the XRD pattern after 50 cycles was very similar to that of the spinel β-$LiFe_5O_8$ (cubic, $a = 8.33$ Å). This means that the orthorhombic Li/$LiFeO_2$ cell is inclined to undergo a structural change during the cycle testing and ultimately reach the spinel phase after long-term cycling. Therefore, we suggest that the main capacity loss of the Li/$LiFeO_2$ cell is based on the structure change from orthorhombic to the spinel phase during cycling. A similar indication has also been reported in the orthorhombic Li/$LiMnO_2$ system. Many research groups proposed that the capacity loss mechanism of the Li/$LiMnO_2$ cell is due to the conversion from the orthorhombic to spinel structure based on various

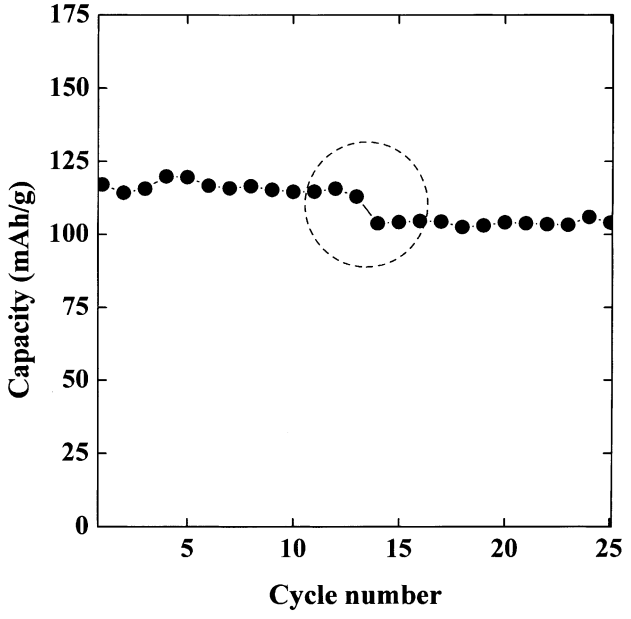

Fig. 4. A plot of the specific discharge vs. number of cycles for the Li/1 M $LiPF_6$–EC/DMC/$LiFeO_2$ system calcined at 150 °C for 15 h in argon. The test condition was a current density of 0.4 mA/cm^2 between 4.5 and 1.5 V at room temperature.

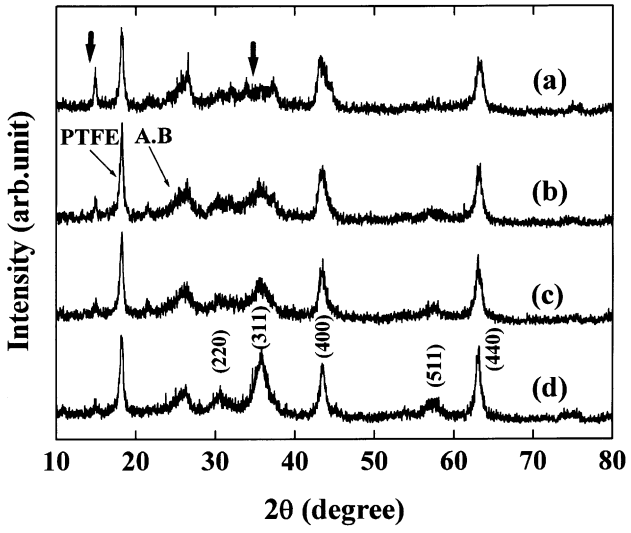

Fig. 5. Ex situ XRD patterns of $LiFeO_2$ electrodes in discharge state after (a) 3th cycle, (b) 10th cycle, (c) 15th cycle, and (d) 50th cycle.

analysis techniques [5,6,18,19]. However, we still have one curiosity about lots of structural transformation in the first cycle, because the almost structural change of the layered cathode materials occurred gradually with cycling. Therefore, we expect that the TEM analysis offers an concrete proof of the capacity loss mechanism in this system as well as the main difference in the electrodes between the 10th and 15th cycles. Further work is now in progress and the results will be reported elsewhere.

4. Conclusion

A well-defined orthorhombic $LiFeO_2$ material has been synthesized at low temperature using a pressing process. It was composed of orthorhombic $LiFeO_2$, small amounts of spinel $LiFe_5O_8$, and defective $LiFeO_2$ phases. The $Li/LiFeO_2$ cell showed not only a fairly high initial discharge capacity over 150 mAh/g, but also a good cycle retention rate at room temperature. It exhibited a very unique characteristic, i.e., a sudden capacity drop near the 13th cycle. We found that orthorhombic $LiFeO_2$ underwent a structural change to the spinel phase during the charge/discharge process and it might be the main reason for the induced capacity loss during the long-term cycling.

Acknowledgements

The authors wish to thank to Ube Chemicals for supplying the electrolyte and support by the High-Tech Research Center Project from the Ministry of Education, Culture, Sports, Science, and Technology.

References

[1] K. Mizushima, P.C. Jones, P.J. Wiseman, J.B. Goodenough, Mater. Res. Bull. 15 (1980) 783.
[2] J.R. Dahn, U. Von Sacken, C.A. Michel, Solid State Ionics 44 (1990) 87.
[3] T. Ohzuku, A. Ueda, M. Nagayama, J. Electrochem. Soc. 140 (1993) 1862.
[4] H. Arai, S. Okada, Y. Sakurai, J. Yamaki, Solid State Ionics 95 (1997) 275.
[5] L. Croguennec, P. Deniard, R. Brec, A. Lecerf, J. Mater. Chem. 5 (1995) 1919.
[6] Y.I. Jang, B. Huang, H. Wang, D.R. Sadoway, Y.M. Chiang, J. Electrochem. Soc. 146 (1999) 3217.
[7] R. Kanno, T. Shirane, Y. Kawamoto, Y. Takeda, M. Takano, M. Ohashi, Y. Yamaguchi, J. Electrochem. Soc. 146 (1996) 2435.
[8] T. Shirane, R. Kanno, Y. Kawamoto, Y. Takeda, M. Takano, T. Kamiyama, F. Izumi, Solid State Ionics 79 (1995) 227.
[9] M. Tabuchi, K. Ado, H. Sakaebe, C. Masquelier, H. Kageyama, O. Nakamura, Solid State Ionics 79 (1995) 220.
[10] M. Tabuchi, C. Masquelier, T. Takeuchi, K. Ado, I. Matsubara, T. Shirane, R. Kanno, S. Tsutsui, S. Nasu, H. Sakaebe, O. Nakamura, Solid State Ionics 90 (1996) 129.
[11] K. Ado, M. Tabuchi, H. Kobayashi, H. Kageyama, O. Nakamura, Y. Inaba, R. Kanno, M. Takagi, Y. Takeda, J. Electrochem. Soc. 144 (1997) L177.
[12] M. Tabuchi, S. Tsutsui, C. Masquelier, R. Kanno, K. Ado, I. Matsubara, S. Nasu, H. Kageyama, J. Solid State Chem. 140 (1998) 159.
[13] M. Tabuchi, K. Ado, H. Kobayashi, I. Matsubara, H. Kageyama, M. Wakita, S. Tsutsui, S. Nasu, Y. Takeda, C. Masqulier, A. Hirano, R. Kanno, J. Solid State Chem. 141 (1998) 554.
[14] Y. Sakurai, H. Arai, S. Okada, J. Yamaki, J. Power Sources 68 (1997) 711.
[15] Y. Sakurai, H. Arai, J. Yamaki, Solid State Ionics 113-115 (1998) 29.
[16] T. Ohzuku, A. Ueda, T. Hirai, Chem. Express 7 (1992) 193.
[17] J.N. Reimers, E.W. Fuller, E. Rossen, J.R. Dahn, J. Electrochem. Soc. 140 (1993) 3396.
[18] L. Croguennec, P. Deniard, R. Brec, J. Electrochem. Soc. 144 (1997) 3323.
[19] Y.S. Lee, M. Yoshio, Electrochem. Solid State Lett. 4 (10) (2001) A166.